

Influence of Annealing Temperatures on the Structural, Morphological, Crystalline and Optical properties of BaTiO₃ and SrTiO₃ Nanoparticles

Mgbemeje EA^{1*}, Akhtar SM^{2,3}, Bong YO^{2,3} and Kue CD⁴

¹Department of Energy Engineering, Chonbuk National University, Republic of Korea

²New & Renewable Energy Material Development Center (NewREC), Chonbuk National University, Jeonbuk, Republic of Korea

³School of Semiconductor and Chemical Engineering, Chonbuk National University, Republic of Korea

⁴Advanced Materials Engineering Department, Chonbuk National University, Republic of Korea

Abstract

In this study, highly crystalline BaTiO₃ and SrTiO₃ nanoparticles were synthesized by bi-modal distribution solution process followed by annealing at different temperatures. The impact of annealing temperatures on the nanoparticles was investigated by their various chemical, structural and surface properties. The particle sizes of both BaTiO₃ and SrTiO₃ increased from 30-80 nm with increase in annealing temperature due to the agglomeration of the nanoparticles. It was found that the optical band gap of BaTiO₃ and SrTiO₃ was considerably decreased with the increase of annealing temperatures from 500 - 900°C. With the observed results, we can say that annealing BaTiO₃ and SrTiO₃ nanoparticles significantly enhance their optical, structural, morphological and crystalline properties.

Keywords: Perovskite materials; Nanoparticles; Optical properties; BaTiO₃; SrTiO₃

Introduction

In this study, highly crystalline BaTiO₃ and SrTiO₃ nanoparticles were synthesized by bi-modal distribution solution process followed by annealing at different temperatures. Perovskite materials with the formula ABO₃ with A being a metal, B, Titanium and O, Oxygen had gained wide attention due to their applications in different technological field [1]. Perovskite generally have a cubic structure with an A site ion usually an alkaline earth or rare earth element, a B site ion located at the center of the lattice and composed generally of either 3d, 4d or 5d transition metal elements [2]. The A atoms are larger than the B atoms and have 12-fold cuboctahedral coordination. The B cation is in a 6-fold coordination surrounded by an octahedron of anions [3]. The relative ion size requirements for stability of the cubic structure of perovskite is quite stringent hence slight buckling and distortion can result in the production of several lower-symmetry distorted perovskite with a reduced A and B cation coordination numbers [4].

Metal oxide perovskite and synthetic perovskite have recently gained wide spread applications in electronics, ceramics, photovoltaic, nanotechnology and biotechnology industries [1]. Synthetic perovskite are currently been applied in high efficient solar cells as a possible less expensive base materials [5]. Barium titanate (BaTiO₃) a ternary perovskite metal oxide is been studied extensively due to its excellent ferroelectric, piezoelectric, dielectric, photo-refractive and superconductive properties [6,7]. Occurring in cubic, tetragonal and orthorhombic phases, BaTiO₃ has shown a wide range of applications in multi-layer ceramic capacitors, positive temperature coefficient devices, piezo-electric sensors, ferroelectric random access memories, printed circuit boards and electro-optical devices [8]. Research on BaTiO₃ shows that the photoluminescence (PL) properties are greatly affected by its growth routes [9]. Strontium titanate (SrTiO₃) perovskite material is a centrosymmetric quantum para-electric material with ferroelectric properties at low temperatures and very high dielectric properties [10]. They are widely used in varistors, advanced ceramics, precision optics, diamond stimulation and in tunable high temperature superconducting microwave filters. Various synthesis routes can be used to synthesize both BaTiO₃ and

SrTiO₃ nanoparticles [11]. Synthesis routes such as electrochemical, hydrothermal [12], sol-gel, solvothermal [13], polymeric precursor and solid state bi-modal distribution methods, play a huge role in the purity and crystallinity of the nanoparticles. The rapid advances in nanotechnology, nanomaterials and nanomechanics offer huge potentials in national defense, homeland security, and private industry. An emphasis on nanoscale entities will make our manufacturing technologies and infrastructure more sustainable in terms of reduced energy usage and environmental pollution. Recent advances in the research community on this topic have stimulated everbroader research activities in science and engineering devoted to their development and their applications. With the confluence of interest in nanotechnology, the availability of experimental tools to synthesize and characterize systems in the nanometer scale, and computational tools widely accessible to model microscale systems by coupled continuum/molecular/quantum mechanics, we are poised to unravel the traditional gap between the atomic and the macroscopic world in mechanics and materials. This in turn opens up new opportunities in education and research.

In this work, BaTiO₃ and SrTiO₃ nanoparticles are synthesized via bi-modal distribution methods followed by annealing at different temperatures of 500 - 900°C and varied annealing times from 1 to 5 h. We investigate the effect of annealing temperature and time on the structural, morphological, optical and crystalline properties of synthesized BaTiO₃ and SrTiO₃ nanoparticles. The detailed properties of BaTiO₃ and SrTiO₃ nanoparticles have been characterized by various experimental characterization tools.

***Corresponding author:** Mgbemeje EA, Department of Energy Engineering, Chonbuk National University, Jeonju, 54896, Republic of Korea, Tel: 821059590434; E-mail: esthermgbemeje@gmail.com

Received May 26, 2016; **Accepted** September 06, 2016; **Published** September 16, 2016

Citation: Mgbemeje EA, Akhtar SM, Bong YO, Kue CD (2016) Influence of Annealing Temperatures on the Structural, Morphological, Crystalline and Optical properties of BaTiO₃ and SrTiO₃ Nanoparticles. J Material Sci Eng 5: 277. doi:10.4172/2169-0022.1000277

Copyright: © 2016 Mgbemeje EA, et al. This is an open-access article distributed under the terms of the Creative Commons Attribution License, which permits unrestricted use, distribution, and reproduction in any medium, provided the original author and source are credited.

Experimental

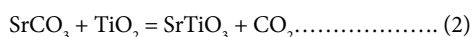
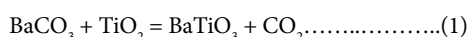
Materials

For the bi-modal distribution method synthesis of BaTiO₃ and SrTiO₃ nanoparticles, Barium carbonate (BaCO₃, sigma aldrich), Strontium carbonate (SrCO₃, sigma aldrich and Titanium (TiO₂ - P-25, sigma aldrich) were used as source materials for Barium, Strontium and Titanium respectively. Distilled water, glass beakers, magnetic stirrers, drying Oven and calcinations machine were also used.

Synthesis of BaTiO₃ and SrTiO₃

The experimental details are presented in the synthesis flow chart, as shown in Figure 1. In brief, the equi-molar BaCO₃/SrCO₃ and TiO₂ powders were mixed together in 10 ml of de-ionized (DI) water in a beaker for 10 minutes. The solutions were stirred for 10 h and the slurry dried in an oven at 80°C for 10 h. After completion of synthesis, the dried powders were annealed at different temperatures and times ranging from 500-900°C and 1-5 h respectively.

The BaTiO₃ and SrTiO₃ chemical reactions can be expressed as follows [14]:



The BaTiO₃ and SrTiO₃ nanoparticles were characterized.

Characterization

X-ray diffraction (XRD) patterns were measured using a Rigaku X-ray Diffractometer operating with Cu K α radiation operating at 40 kV and 30 mA and the scans rates were carried out at 0.02° at 10° min⁻¹ in a 2 θ range from 20° to 70°. Particle surface morphology was carried out via HITACHI Su-70 Field Emission Scanning Electron Microscope (FESEM). Element analysis was carried out via an AMETEK EDAX with a 10 mm² active area. The particle size, shape and morphology were also analyzed using a JEOL JEM 2010 Transmission Electron Microscope operating at 200 Kv. The particles surface areas were determined via Brunauer-Emmett-Teller (BET) test and Raman Spectroscopy was performed using a Nanofinder 30 Tokyo-Raman model with a 488 nm laser, a 1.0 mW laser power, a 5 second exposure, a 50X objective lens and a 600 Gmm grating. UV-vis spectra were measured by a JASCO V-670 spectrophotometer at a scan speed of 1000 nm/min and a UV-vis bandwidth of 0.2 nm and data interval of 1.0 nm.

Results and Discussion

The crystalline nature of synthesized BaTiO₃ and SrTiO₃

nanoparticles has been examined by the XRD patterns. Figures 2 and 3 show the XRD patterns of BaTiO₃ and SrTiO₃ nanoparticles at different temperatures and times. BaTiO₃ and SrTiO₃ present the main diffraction peak at 32.3° (110), indicating the formation of perovskite materials. It can be seen that the intensity of diffraction peak at 22.4° (100) in both materials is drastically decreased with the increase of annealing temperature. The observed XRD peaks in Figures 2 and 3 confirm that BaTiO₃ and SrTiO₃ nanoparticles possess the cubic and tetragonal phases. Noticeably, the diffraction peak intensities also change markedly with an elevation of the annealing temperatures [15,16].

The strong and sharp diffraction peaks in Figures 2 and 3 suggest that BaTiO₃ and SrTiO₃ nanoparticles have good crystalline nature. At high annealing temperatures (800 and 900°C), no diffraction peaks are seen for carbonates, confirming the complete removal of BaCO₃ and SrCO₃ impurities. Moreover, the high peak intensity at higher annealing temperature is related to the reduction of the hydroxyl (OH) on the BaTiO₃ and SrTiO₃ unit cells in a lattice defect of their cubic structures.

The UV-Vis absorption spectra of BaTiO₃ and SrTiO₃ nanoparticles are shown in Figures 4 and 5. The maximum absorption peaks in BaTiO₃ and SrTiO₃ nanoparticles are positively shifted with the variation of annealing temperatures. The optical band gaps were calculated using the maximum absorbance in UV-vis spectra. The calculated band gaps with different annealing temperatures at 500, 600, 700, 800, and 900°C are 3.88 eV, 3.86 eV, 3.75 eV, 3.52 eV, 3.47 eV for BaTiO₃ and 3.73 eV, 3.71 eV, 3.66 eV and 3.43 eV for SrTiO₃ at 500, 600°C, 700°C and 900°C respectively. The absorption peak shifting indicates that the optical properties of BaTiO₃ and SrTiO₃ nanoparticles are changed by the variation of annealing temperatures and time.

The Optical absorption spectrum of BaTiO₃ nanoparticles revealed that the particles were transparent in the visible region. The electron transition types and band structure were analyzed via the dependence of optical absorption coefficient on photon energy.

Figures 6 and 7 shows the FESEM micrographs of BaTiO₃ and SrTiO₃ nanoparticles to explain the morphological changes upon the annealing. From Figure 6, the particles sizes are increased and agglomerated with the increase of annealing temperatures from 500-900°C. Figure 7 also presents the similar morphological changes as the increase of annealing temperatures. At low annealing temperature, small cluster of particles are visible. However, the less clustered spherical cubic nanoparticles are observed at 800°C and 900°C annealing temperature. The particle sizes of 32 nm at 500°C show a steady increase in particle size to 80 nm at 900°C. This sharp increase in size might occur due to sintering effect at high temperature.

A JEM 2010 Transmission electron microscope was used to measure the size and morphology of both nanoparticles. The TEM image measure via a bright-field low magnification revealed that both BaTiO₃ and SrTiO₃ nanoparticles are spherical in shape while the Selective Area Electron Diffraction Pattern (SAED) showed the presence of polycrystalline diffraction rings composed of continuous discrete diffraction dots in both nanoparticles although more diffraction rings are observed in BaTiO₃ nanoparticles. The average estimated particle size of SrTiO₃ and BaTiO₃ was 37 and 38 nm respectively. The TEM images are shown in Figure 8. The chemical compositions and elemental analysis were measured via EDX and the results depicted in the Figures 9 and 10. Both spectra show Ba, Sr and Ti peaks along with O peak. The existence of these elements in the synthesized samples confirms the formation of BaTiO₃ and SrTiO₃. The appearance of C peak suggests the presence of carbonate traces.

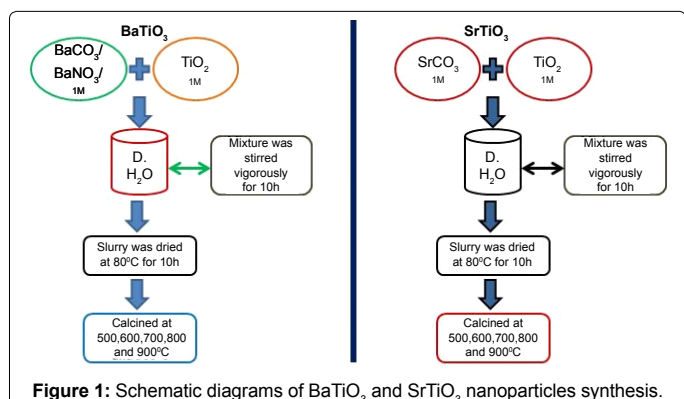


Figure 1: Schematic diagrams of BaTiO₃ and SrTiO₃ nanoparticles synthesis.

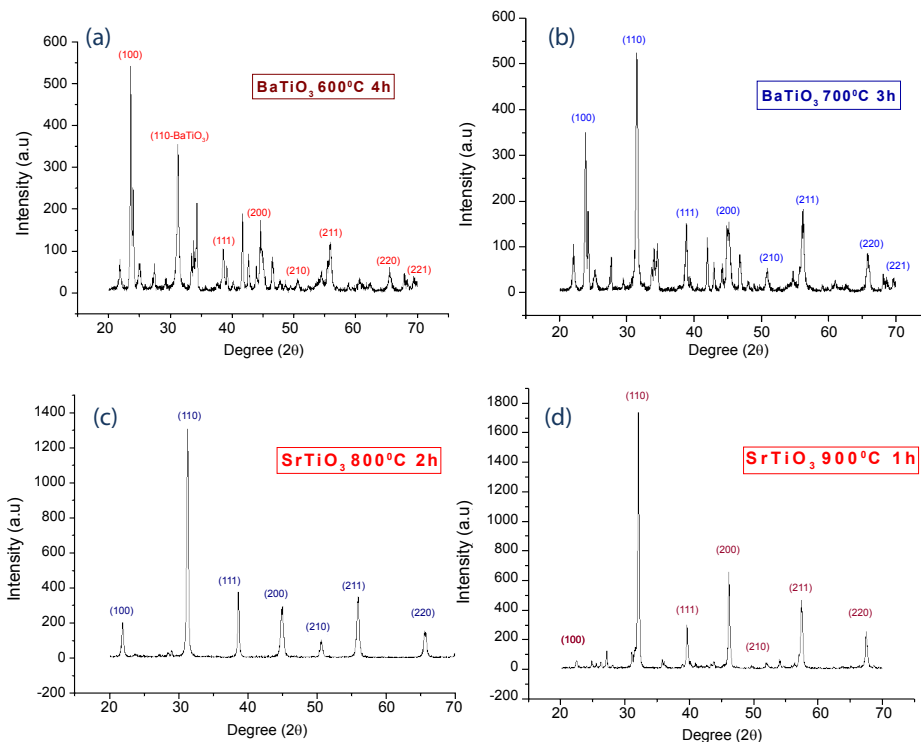


Figure 2: XRD peak patterns for BaTiO₃ nanoparticles synthesized at different annealing temperatures and time. (a) 600°C 4h, (b) 700°C 3h, (c) 800°C 2h and (d) 900°C 1h.

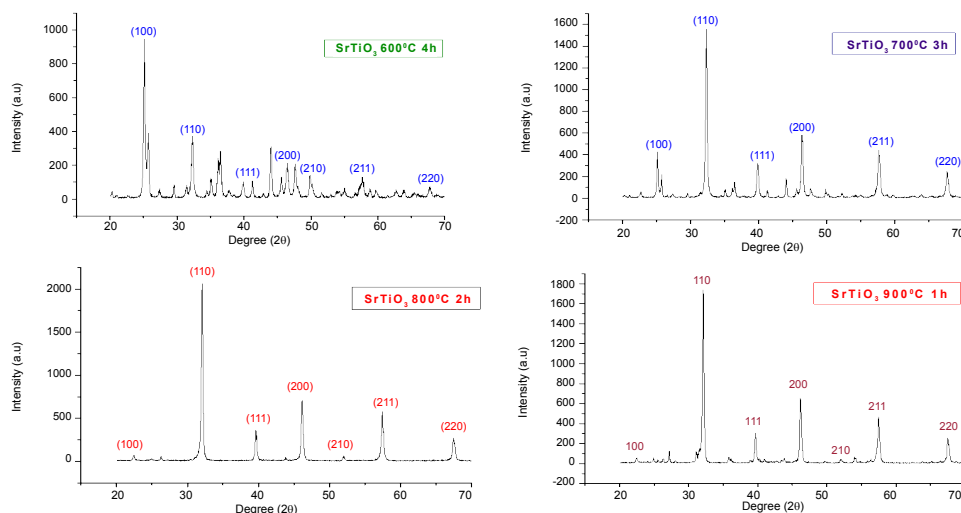
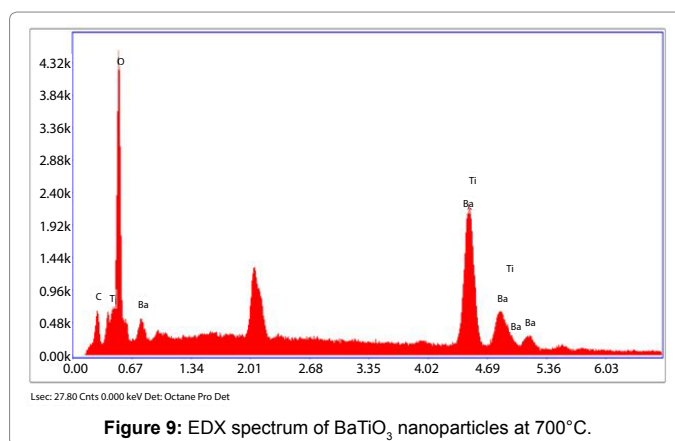
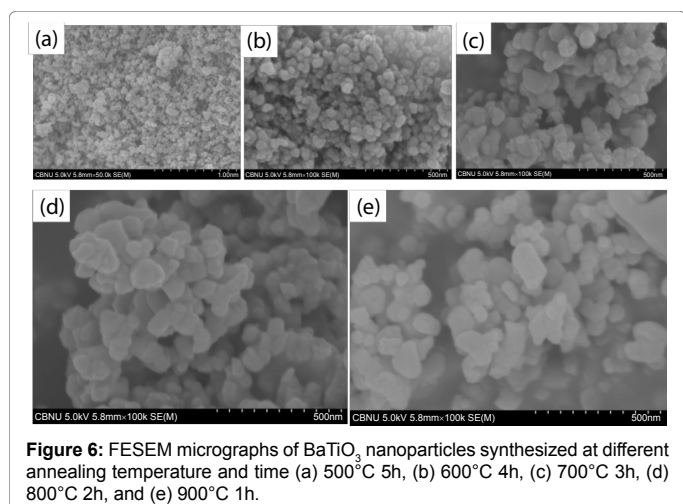
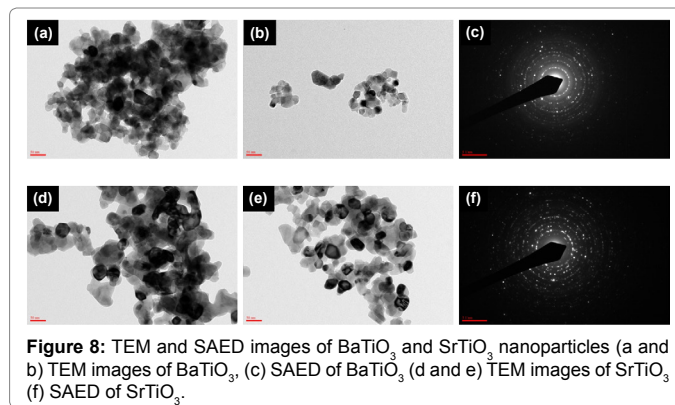
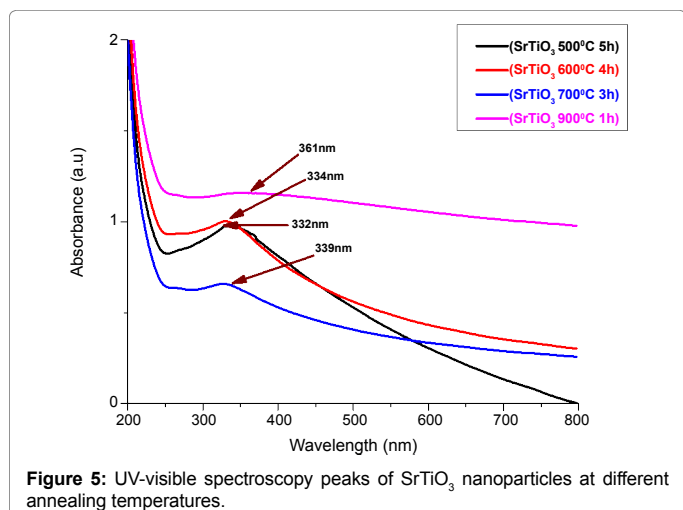
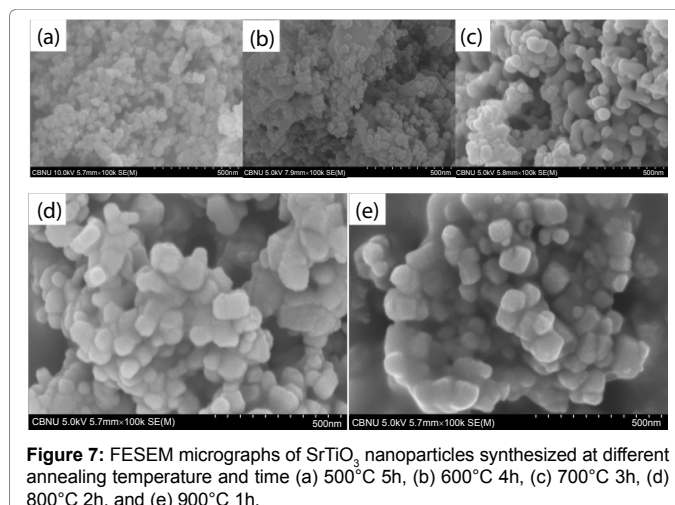
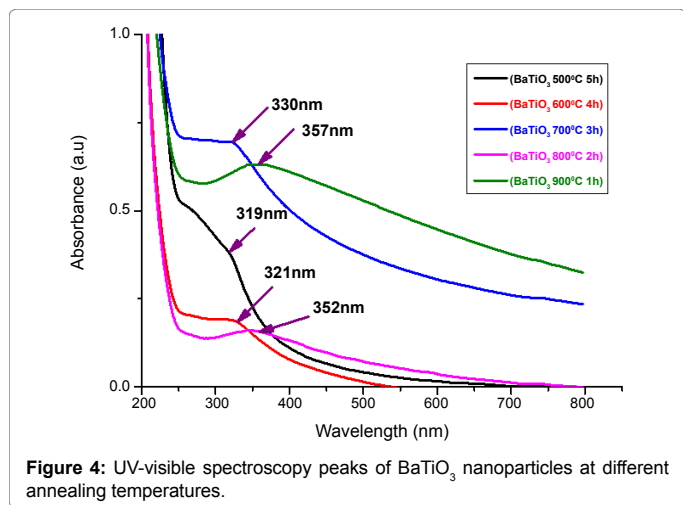


Figure 3: XRD peak patterns for SrTiO₃ nanoparticles synthesized at different annealing temperatures and time. (a) 600°C 4h, (b) 700°C 3h, (c) 800°C 2h and (d) 900°C 1h.

The Raman spectra of BaTiO₃ nanoparticles are represented in Figure 11. BaTiO₃ nanoparticles exhibit the several Raman bands centered at 247, 253, 254, 261 and 517 cm⁻¹ peaks, which are in conformation with reported peak ranges of ~285-520 cm⁻¹. These bands are associated to the displacement of Ti⁴⁺ ions at high temperatures. The Raman bands at 304, 307, 395, 639 and 712 cm⁻¹ are the indicative of the presence of tetragonal BaTiO₃ phases [9]. Small Raman band at 1058 cm⁻¹ represents the presence of some BaCO₃ impurities in BaTiO₃ samples annealed at 600, 700, 800°C while Raman bands at 805 and 856 cm⁻¹ for BaTiO₃ samples annealed at 900°C are related to the oxygen deficiencies. The

observed Raman bands are consistent with the standard peaks reported for BaTiO₃ [17]. The appearance of Raman bands at 712 cm⁻¹ and 304 cm⁻¹ can be attributed to the highest longitudinal optical mode with A₁ symmetry and the B₁ mode indicating the presence of asymmetry within the TiO₆ octahedra of BaTiO₃, respectively.

Figure 12 shows the Raman spectra of synthesized SrTiO₃ nanoparticles. In general, bulk SrTiO₃ particles exhibit a centrosymmetric cubic structure at room temperature, as a result, the first order Raman scattering peaks are not observed. From Figure 11,



SrTiO₃ nanoparticles obtain the first order peaks at 152, 182, 183, 187 and 518 cm⁻¹. The Raman shifts at 152 and 182 cm⁻¹ can be ascribed to the band gap (E_g) mode of non-centrosymmetric [18] while, the latter two peak modes (183 and 187 cm⁻¹) is resulted from the polar TO₂ and TO₄ phonons. SrTiO₃ nanoparticles present few second order Raman peaks at 292, 301, 397, 629, 637, 645 cm⁻¹ peaks [4,19], indicating the

formation of SrTiO₃. Moreover, the Raman peaks at 1028, 1292 and 1610 cm⁻¹ belong to the carbonate (SrCO₃) impurities in samples, respectively.

The BET and Langmuir surface area of synthesized BaTiO₃ and SrTiO₃ nanoparticles are lowered with the increase of annealing temperatures from 600 to 700°C. In general, the particle BET was measured from the N₂ adsorption/desorption isotherms at 77.35 K.

The surface to volume properties of synthesized BaTiO₃ and SrTiO₃ nanoparticles have been analyzed by measuring the BET specific surface areas (S_{BET}). The surface properties results are summarized in Table 1.

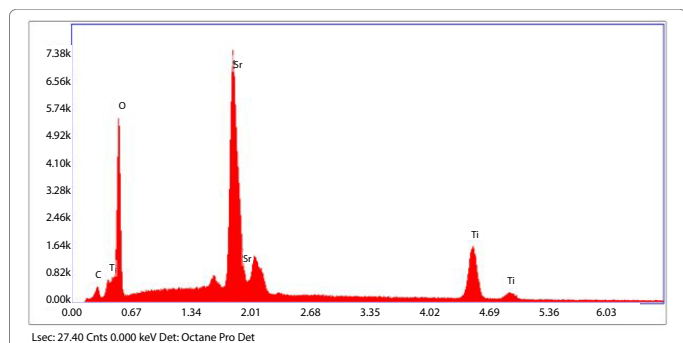


Figure 10: EDX Spectrum of SrTiO₃ nanoparticles at 700°C.

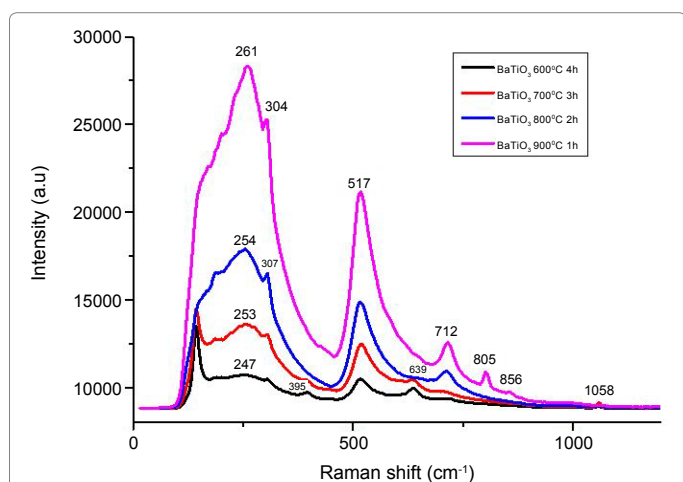


Figure 11: Raman Spectra of BaTiO₃ nanoparticles at different annealing temperatures of 600, 700, 800 and 900°C.

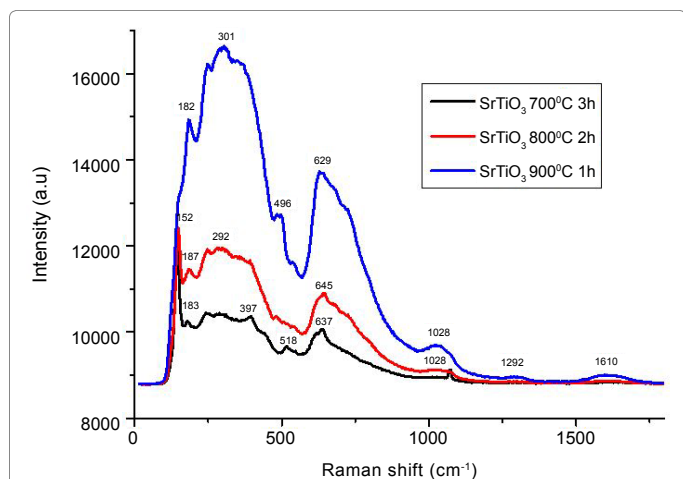


Figure 12: Raman Spectra of SrTiO₃ nanoparticle at different annealing temperatures of 600, 700, 800 and 900°C.

Sample name/ Temp(°C)	BET Surface Area (m ² g)	Langmuir Surface Area (m ² g)	dBET (nm)
BaTiO ₃ - 600	16.70	23.82	59.7
BaTiO ₃ - 700	11.00	15.60	90.6
SrTiO ₃ - 600	18.49	26.39	67.0
SrTiO ₃ - 700	16.80	23.96	74.0

Table 1: BET and dBET surface areas of BaTiO₃ and SrTiO₃ annealed at 600°C and 700°C.

It is assumed that internal pores are absent from the powders, then the average particle sizes of both powders are calculated via the following formula;

$$dBET = 6/(\rho \times S_{BET})$$

Where ρ is the theoretical density of BaTiO₃ which is 6.017 g/cm³ and that of SrTiO₃ is 4.81 g/cm³ [11]. The estimated results are shown in Table 1 above. The average particle sizes are increased with the increase of annealing temperature. The estimated values are in excellent with the particle sizes observed in FESEM results. The decrease in surface area at high annealed temperature is usually associated to the removal of surface hydroxyl group on BaTiO₃ and SrTiO₃ nanoparticles, which might cause the agglomeration of particles.

Conclusion

BaTiO₃ and SrTiO₃ nanoparticles were successfully synthesized by bi-modal distribution solution and which performed the annealing at different temperatures ranging from 500-900°C. The morphological observations shown that BaTiO₃ and SrTiO₃ nanoparticles increase with increase in annealing temperature. The cubic and tetragonal phases of BaTiO₃ and SrTiO₃ perovskites were deduced by the XRD and Raman spectra studies. The optical band gap varied from 3.88-3.47 eV for BaTiO₃ and 3.73- 3.43 eV for SrTiO₃ as the annealing temperature increased. Surface properties shows that the surface areas of BaTiO₃ and SrTiO₃ nanoparticles gradually decreased as the annealing temperature increased from 500 to 900°C. From this study, we can conclude that both BaTiO₃ and SrTiO₃ nanoparticles showed similar impact on annealing temperature in terms of their morphological, structural, crystalline and optical properties.

Acknowledgement

This work was supported by the Energy Efficiency and Resources of the Korean Institute of Energy Technology Evaluation and Planning (KETEP) grant funded by the Korea government Ministry of knowledge Economy (NO. 2013T100200119).

References

- Chien AT, Xu X, Kim JP, Lange FF (1999) Electrical characterization of BaTiO₃ heteroepitaxial thin films by hydrothermal synthesis. J Mater Res 14: 3330-3339.
- Raveau B (2007) The perovskite history: More than 60 years of research from the discovery of ferroelectricity to colossal magnetoresistance via high T-C superconductivity - preface. Prog Solid State Chem 35: 171-173.
- Fuentes S, Muñoz P, Barraza N, Chávez-Ángel E, Sotomayor Torres CM (2015) Structural characterisation of slightly Fe-doped SrTiO₃ grown via a sol-gel hydrothermal synthesis. J Sol-Gel Sci Technol 75: 593-601.
- Johnston K, Huang X, Neaton JB, Rabe KM (2005) First-principles study of symmetry lowering and polarization in BaTiO₃/SrTiO₃ superlattices with in-plane expansion. Physical Review B 71.
- Kato Y (2015) Silver iodide formation in methyl ammonium lead iodide perovskite solar cells with silver top electrodes. Adv Mater Interfaces 2: 1500195.
- Kamalasanan MN, Chandra S, Joshi PC, Mansingh A (1991) Structural and optical-properties of sol-gel-processed BaTiO₃ Ferroelectric Thin-Films. Appl Phys Lett 59: 3547-3549.
- Marquez-Herrera A (2012) Effect of substrate temperature on the structural properties, optical and ferroelectric BaTiO₃ thin films deposited by RF sputtering. Revista Mexicana De Fisica 58: 308-312.
- Mao YB, Banerjee S, Wong S (2003) Hydrothermal synthesis of BaTiO₃ and SrTiO₃ nanotubes. Abstracts of Papers of the American Chemical Society 226: U690-U690.
- Zhan H, Xiangping J, Mianxia Z, Xiaohong L, Zhiyun L (2016) Photoluminescence activity of BaTiO₃ nanocrystals dependence on the structural evolution. Journal of Crystal Growth 433: 80-85.

10. Huang ST, William Lee WL, Chang JL, Chen CC (2014) Hydrothermal synthesis of SrTiO₃ nanocubes: Characterization, photocatalytic activities, and degradation pathway. Journal of the Taiwan Institute of Chemical Engineers 45: 1927-1936.
11. Zeng M (2011) Surface reaction characteristics at low temperature synthesis BaTiO₃ particles by barium hydroxide aqueous solution and titanium tetraisopropoxide. Appl Surf Sci 257: 6636-6643.
12. Zhang YF, Xu G, Wei X, Ren ZH, Liu Y, et al. (2012) Hydrothermal synthesis, characterization and formation mechanism of self-assembled mesoporous SrTiO₃ spheres assisted with Na₂SiO₃ center dot 9H(2)O. CrystEngComm 14: 3702-3707.
13. Xu G, Tao Z, Zhao Y, Zhang Y, Ren Z (2013) Solvothermal synthesis, characterization and formation mechanism of single-crystalline SrTiO₃ dense spheres with monoethanolamine as reaction medium solvent. CrystEngComm 15: 1439-1444.
14. Manzoor U, Kim DK (2007) Synthesis of nano-sized barium titanate powder by solid-state reaction between barium carbonate and titania. J Mater Sci Technol 23: 655-658.
15. Ren XC, Nie WL, Bai Y, Qiao LJ (2015) Effect of sintering temperature and oxygen atmosphere on electrocaloric effect of BaTiO₃ ceramics. European Physical Journal B 88: 232.
16. Saleem M, Song JS, Kim I, Jeong SJ (2015) effect of sintering temperature on electrical and dielectric properties of Ni based BaTiO₃ composite. Journal of Nanoelectronics and Optoelectronics 10: 386-390.
17. Chinchamalature VR, Ghosh SA, Chaudhari GN (2010) Synthesis and electrical characterization of BaTiO₃ thin films on Si(100). Materials Sciences and Applications 1: 187-190.
18. Sirenko AA, Akimov IA, Fox J, Xi XX (1999) Observation of the first-order Raman scattering in SrTiO₃ thin films. Phys Rev Lett 82: 4500-4503.
19. Maddaiah M, Babu Naidu KC, Rani DJ, Subbarao T (2015) Synthesis and characterization of Cuo-Doped SrTiO₃ ceramics. Journal of Ovonic Research 11: 99-106.